Supplementary Material

Sulfonate Compounds Embraced from *Acid* Copper Electroplating Baths as Innovative Additives in *Alkaline* Zn Batteries

Katerina Bogomolov [1], Ekaterina Grishina [1] and Yair Ein-Eli [1,2,]*

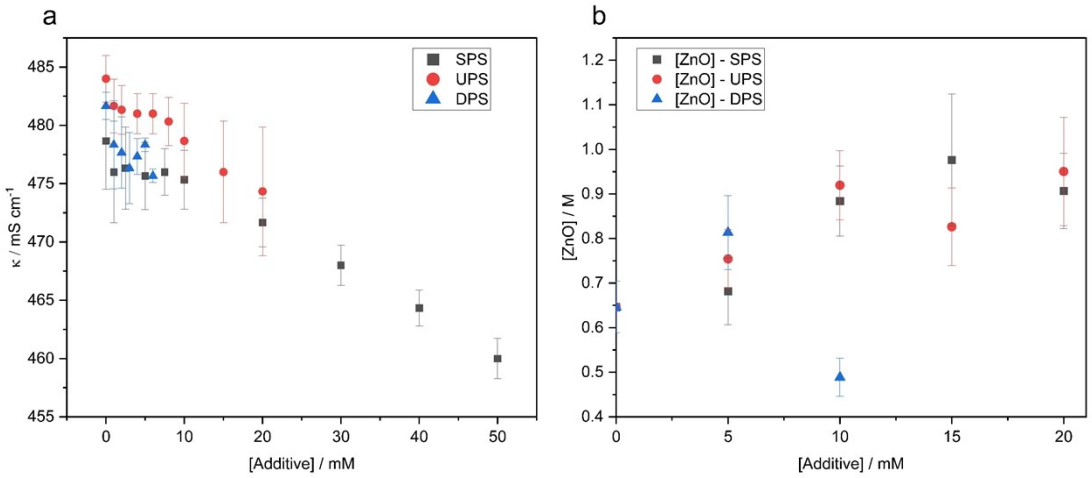

Supplementary Figure 1. (a) Conductivity of SPS-, UPS- and DPS- modified alkaline electrolyes (5M KOH + 0.3M ZnO); (b) Solubility limits of ZnO in alkaline electrolyes modified by different concentrations of SPS, UPS and DPS.

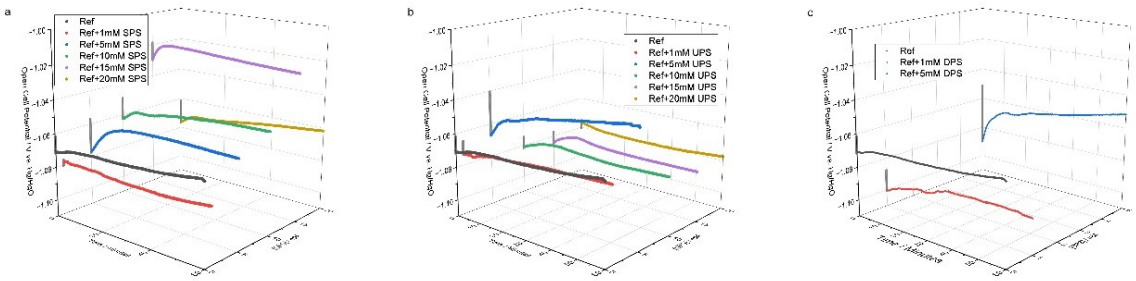

Supplementary Figure 2. Open cell potentials of Sn substrate measured vs. Hg/HgO reference electrode in additive-free (5M KOH + 0.3M ZnO) and additive-modified electrolytes: (a) SPS; (b) UPS and (c) DPS.

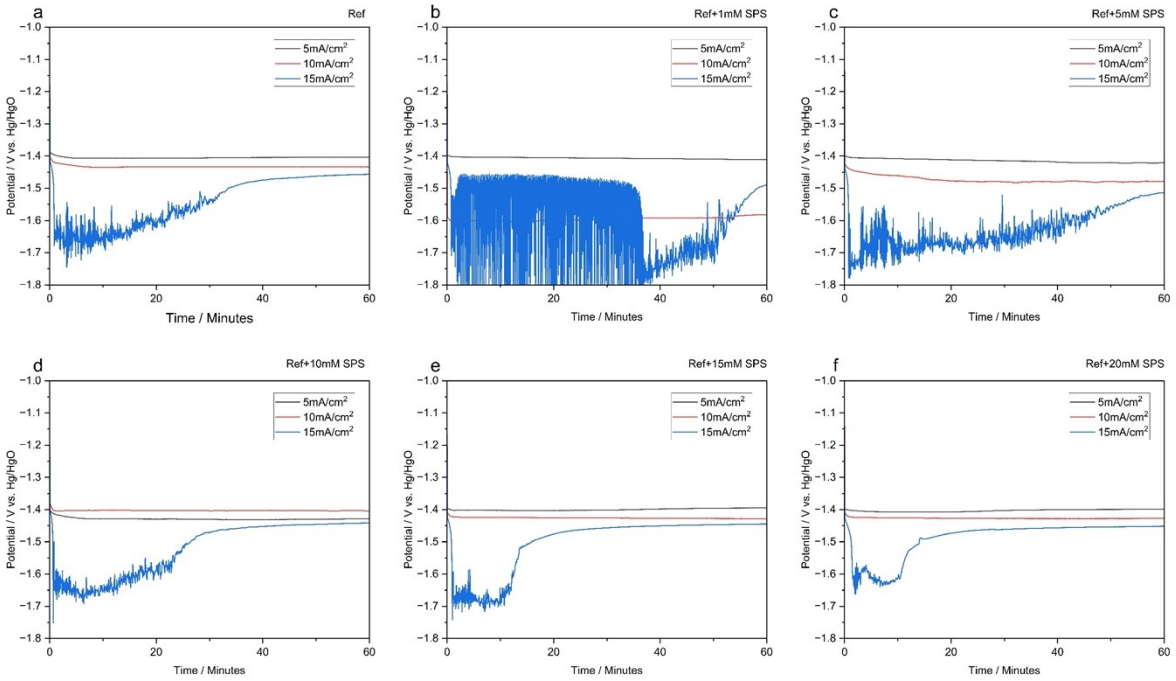

Supplementary Figure 3. Chronopotentiometry profiles obtained at current densities of 5, 10 and 15 mA cm^{-2} in: (a) additives-free electrolyte, and (b-f) SPS-modified electrolyte; (b) 1mM SPS; (c) 5mM SPS; (d) 10mM SPS; (e) 15mM SPS, and (f) 20mM SPS.

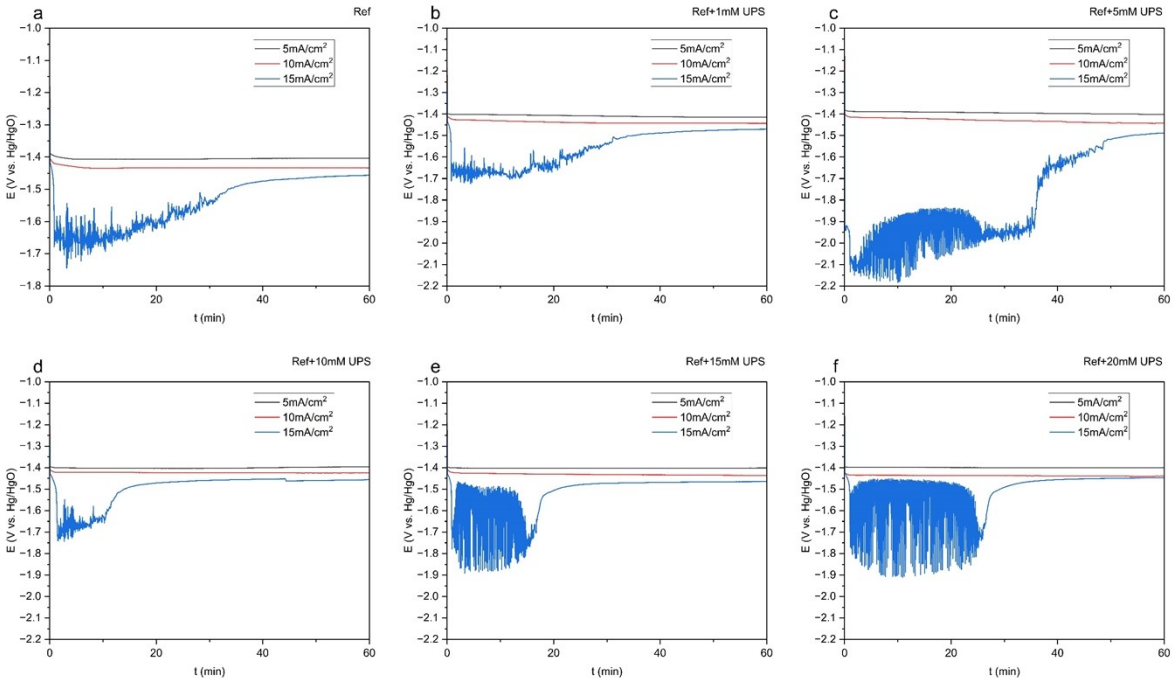

Supplementary Figure 4. Chronopotentiometry profiles obtained at current densities of 5, 10 and 15 mA cm^{-2} in: (a) additive-free electrolyte, and (b-f) UPS-modified electrolyte; (b) 1mM UPS, (c) 5mM UPS, (d) 10mM UPS, (e) 15mM UPS and, (f) 20mM UPS.

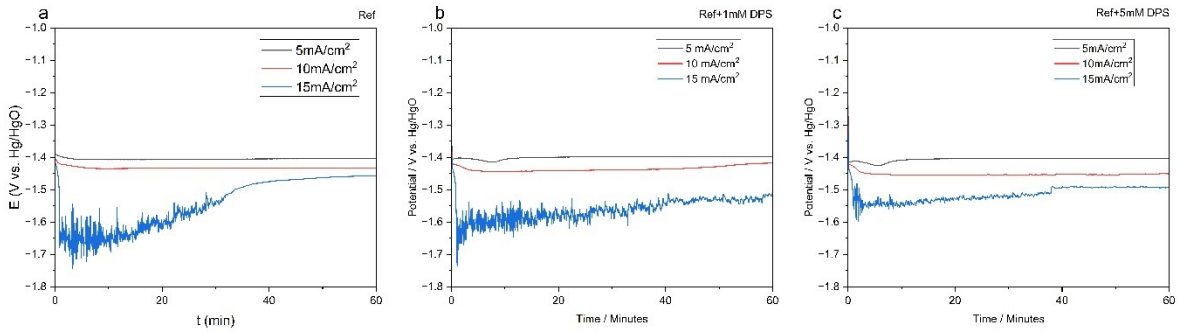

Supplementary Figure 5. Chronopotentiometry profiles obtained at current densities of 5, 10 and 15 mA cm^{-2} in (a) additive-free electrolyte, and (b, c) DPS-modified electrolyte: (b) 1mM DPS; (c) 5mM DPS.

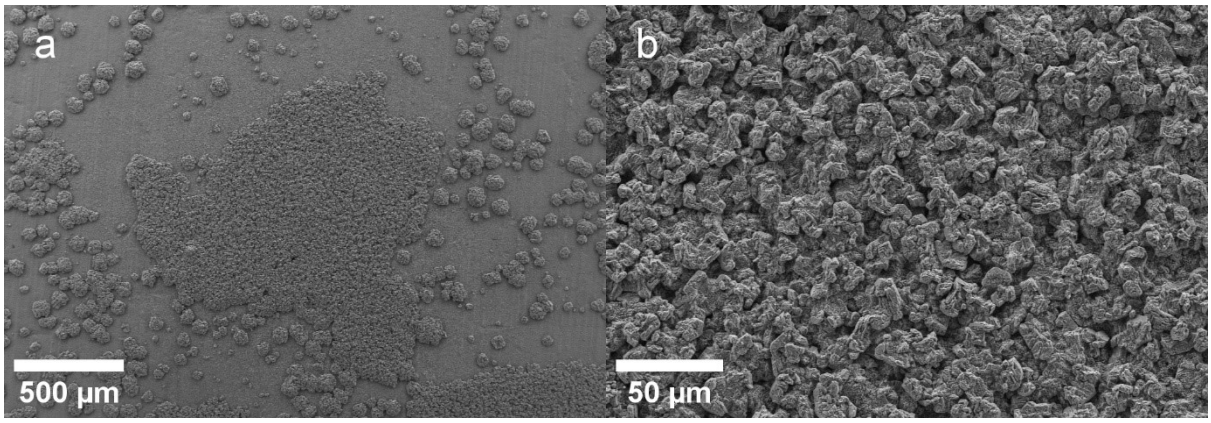

Supplementary Figure 6. SEM micrographs of Zn deposited from a Ref solution [an additives-free electrolyte (5.0M KOH, 0.3M ZnO)] over Sn current collector at current density of **5 mA cm^{-2}** for 1h; taken at magnifications of (a) X100 and (b) X1000.

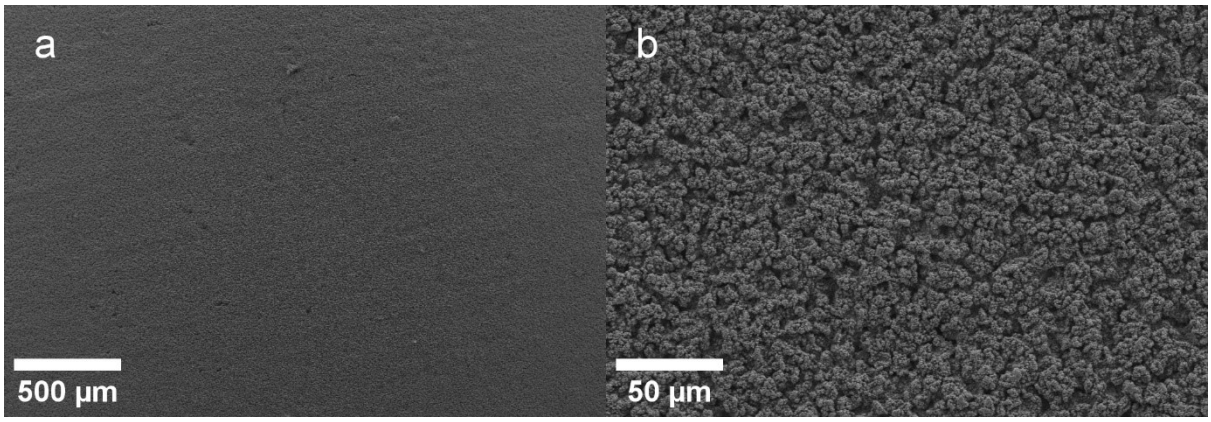

Supplementary Figure 7. SEM micrographs of Zn deposited from a Ref solution [an additives-free electrolyte (5.0M KOH, 0.3M ZnO)] over Sn current collector at current density of **10 mA cm^{-2}** for 1h; taken at magnifications of (a) X100 and (b) X1000.

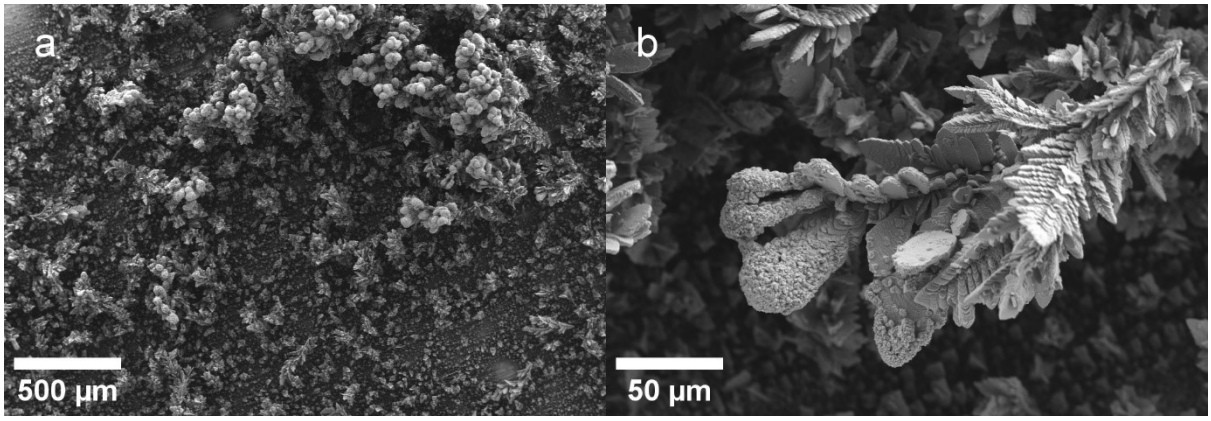

Supplementary Figure 8. SEM micrographs of Zn deposited from a Ref solution [an additives-free electrolyte (5.0M KOH, 0.3M ZnO)] over Sn current collector at current density of 15 mA cm^{-2} for 1h; taken at magnifications of (a) X100 and (b) X1000.

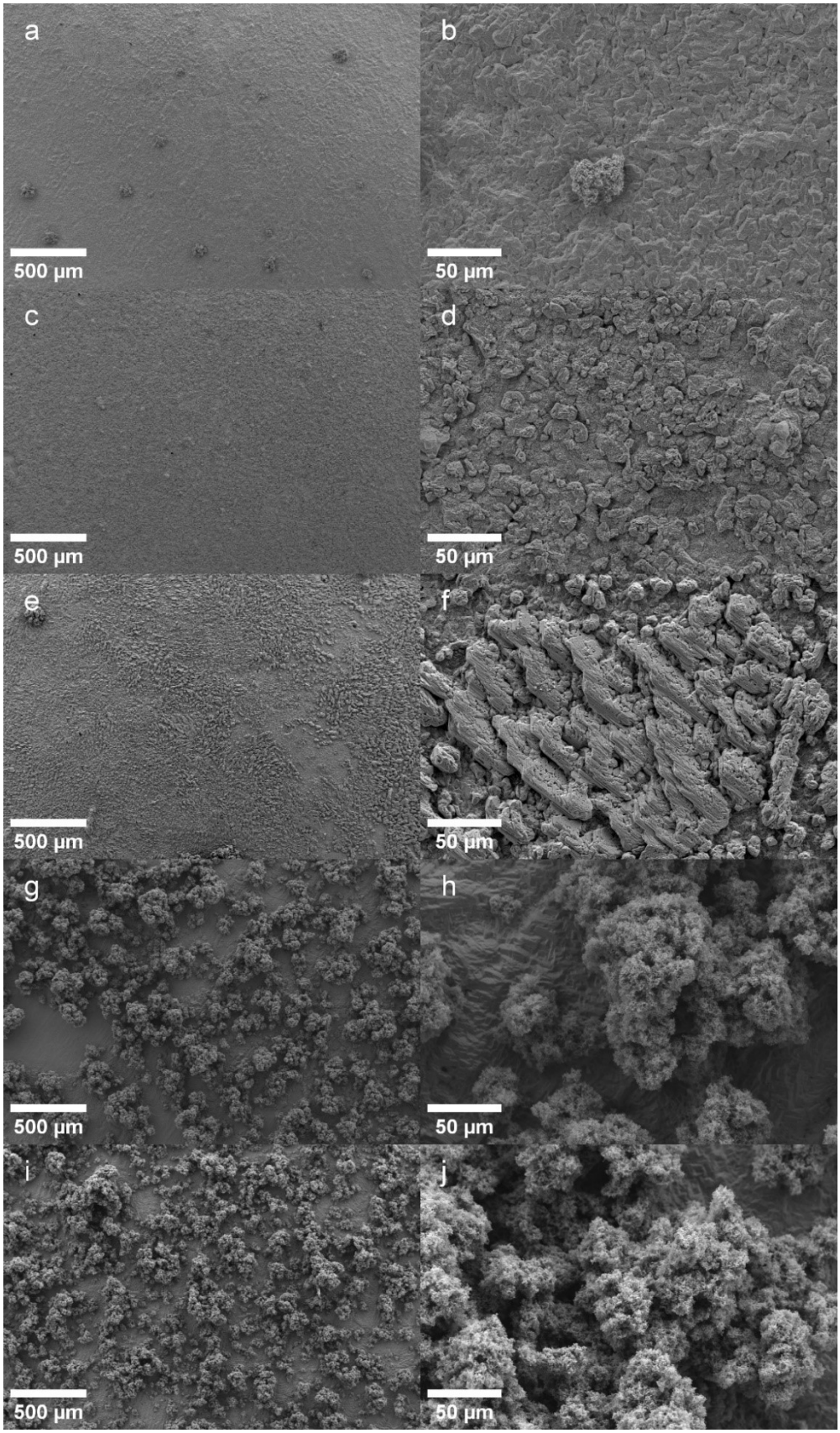

Supplementary Figure 9. SEM micrographs of Zn deposited over Sn current collector at a current density of **5 mA cm^{-2}** for 1h, taken at X100 and X1000 magnifications, respectively: (a)+(b) from Ref+1mM SPS solution; (c)+(d) Ref+5mM SPS solution; (e)+(f) Ref+10mM SPS solution; (g)+(h) Ref+15mM SPS solution; (i)+(j) Ref+20mM SPS solution.

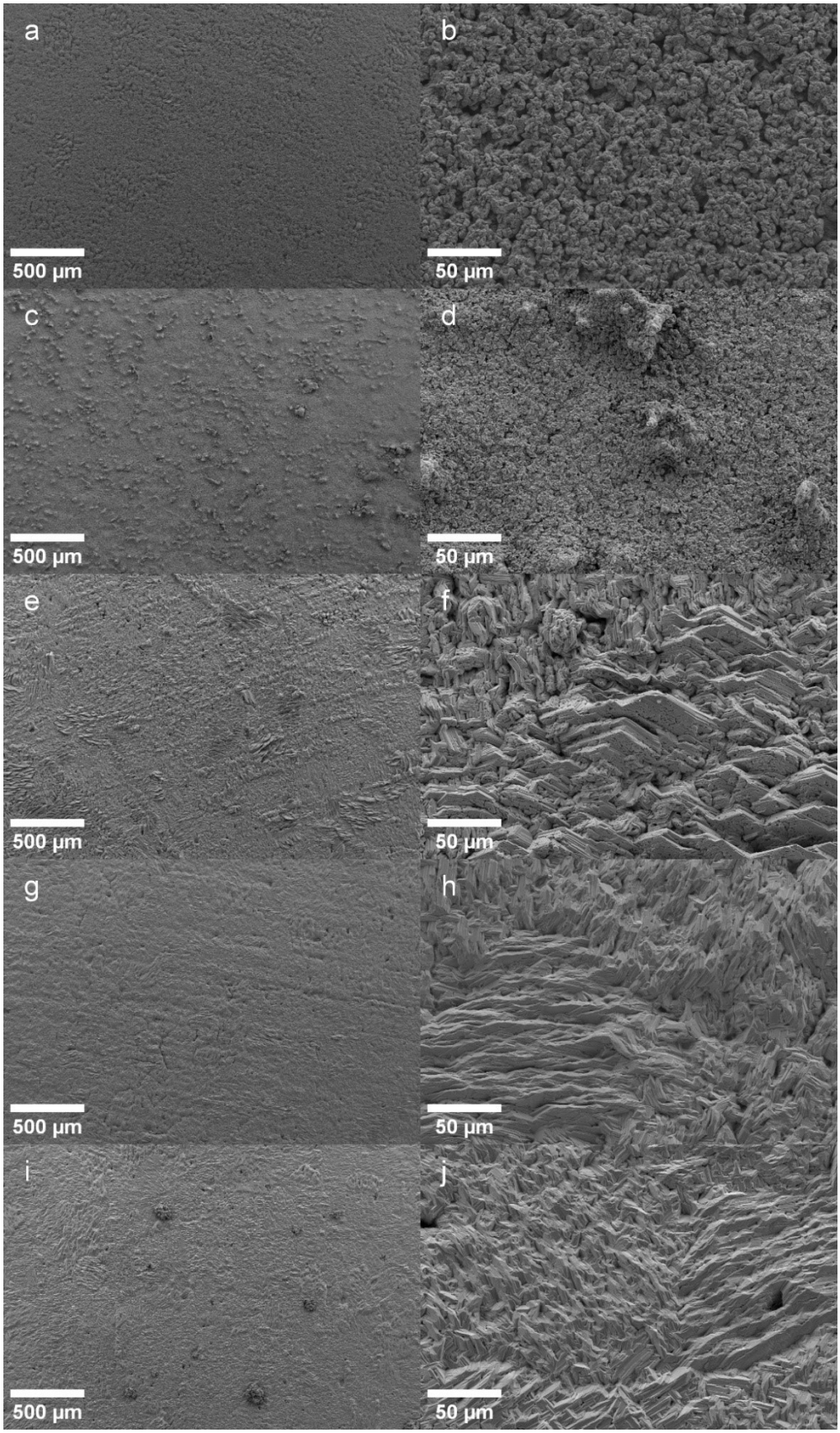

Supplementary Figure 10. SEM micrographs of Zn deposited over Sn current collector at a current density of **10 mA cm^{-2}** for 1h, taken at X100 and X1000 magnifications, respectively: (a)+(b) from Ref+1mM SPS solution; (c)+(d) Ref+5mM SPS solution; (e)+(f) Ref+10mM SPS solution; (g)+(h) Ref+15mM SPS solution; (i)+(j) Ref+20mM SPS solution.

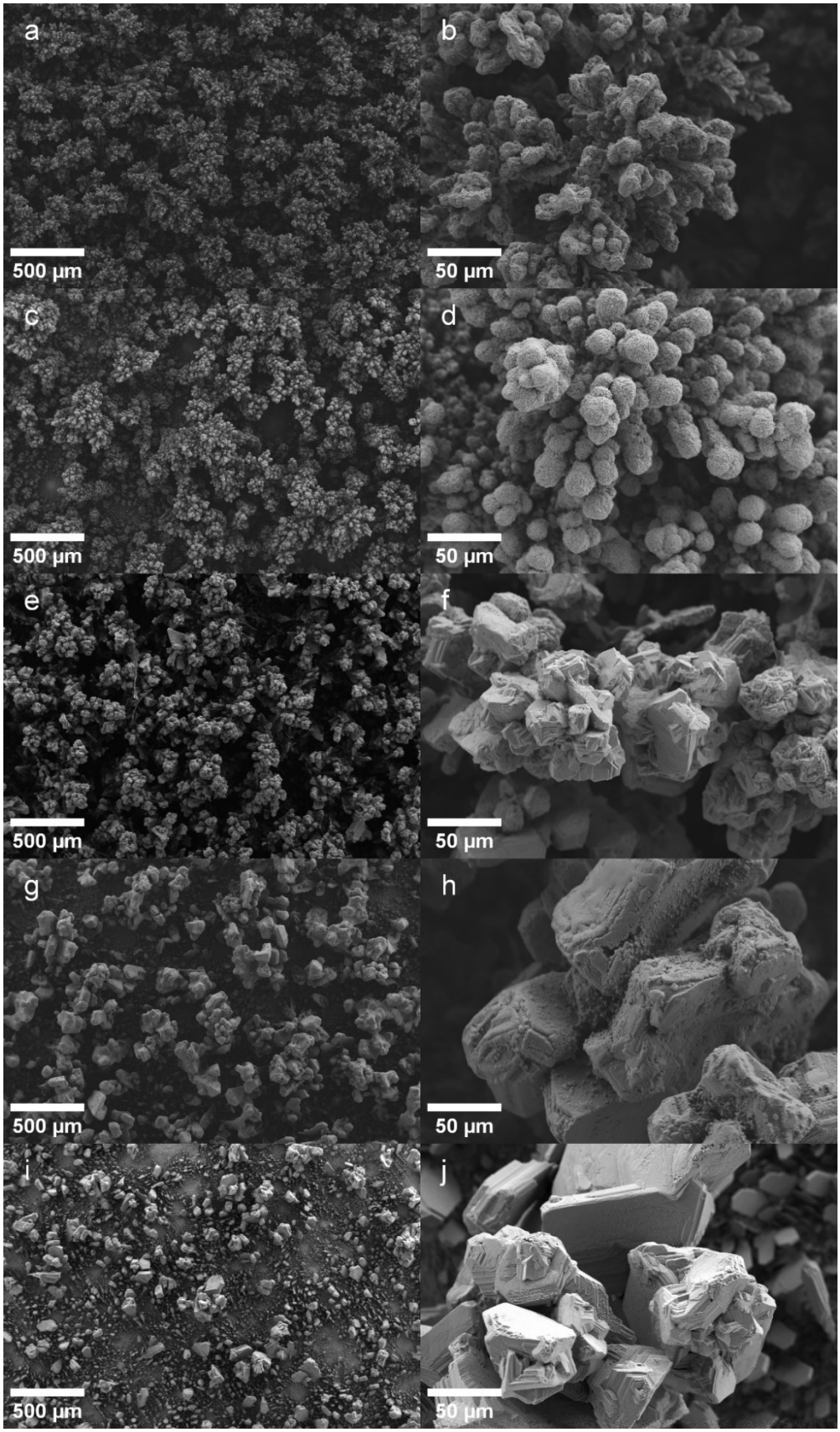

Supplementary Figure 11. SEM micrographs of Zn deposited over Sn current collector at a current density of **15 mA cm^{-2}** for 1h, taken at X100 and X1000 magnifications, respectively: (a)+(b) from Ref+1mM SPS solution; (c)+(d) Ref+5mM SPS solution; (e)+(f) Ref+10mM SPS solution; (g)+(h) Ref+15mM SPS solution; (i)+(j) Ref+20mM SPS solution.

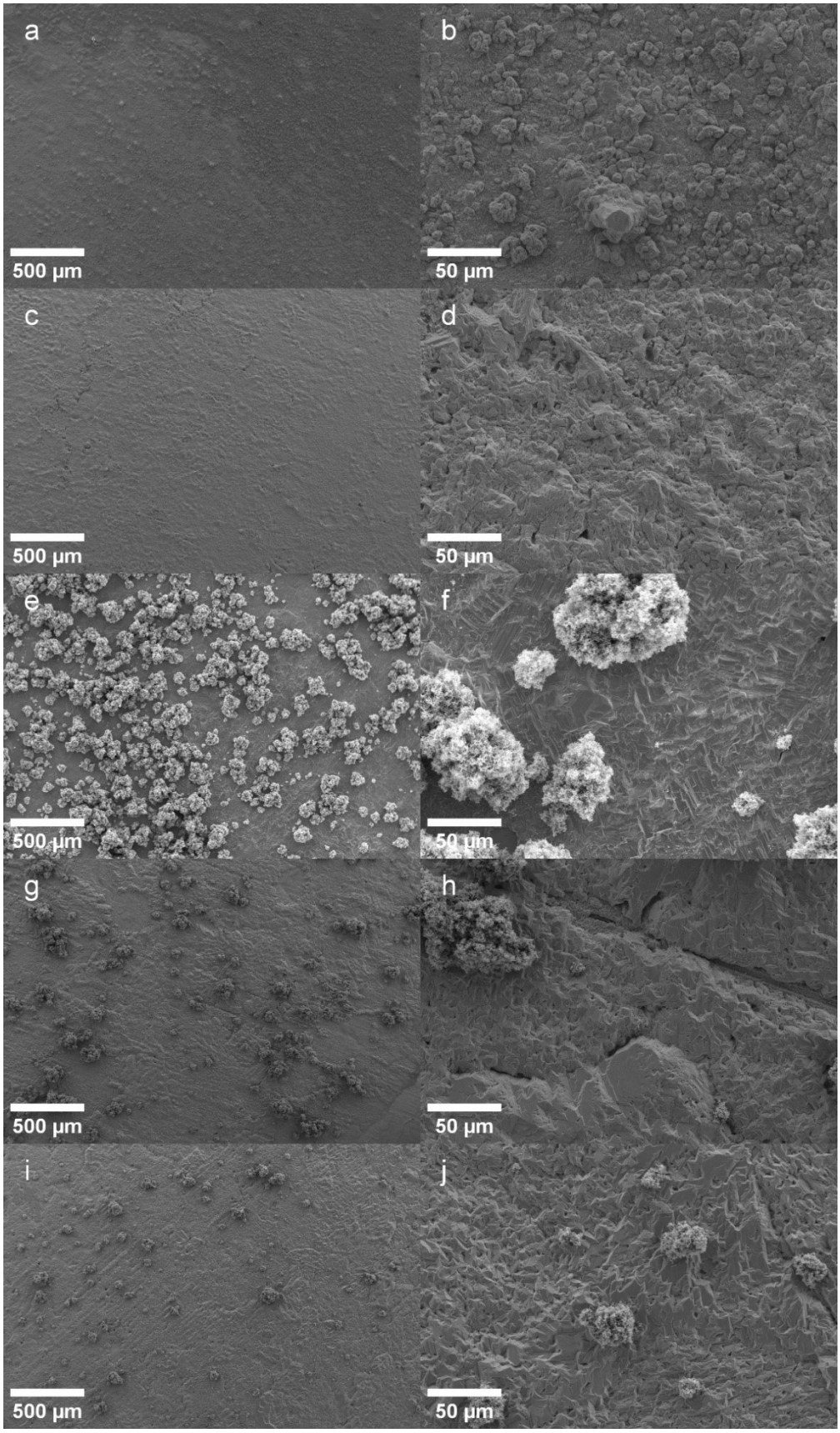

Supplementary Figure 12. SEM micrographs of Zn deposited over Sn current collector at a current density of **5 mA cm^{-2}** for 1h, taken at X100 and X1000 magnifications, respectively: from (a)+(b) Ref+1mM UPS solution; (c)+(d) Ref+5mM UPS solution; (e)+(f) Ref+10mM UPS solution; (g)+(h) Ref+15mM UPS solution; (i)+(j) Ref+20mM UPS solution.

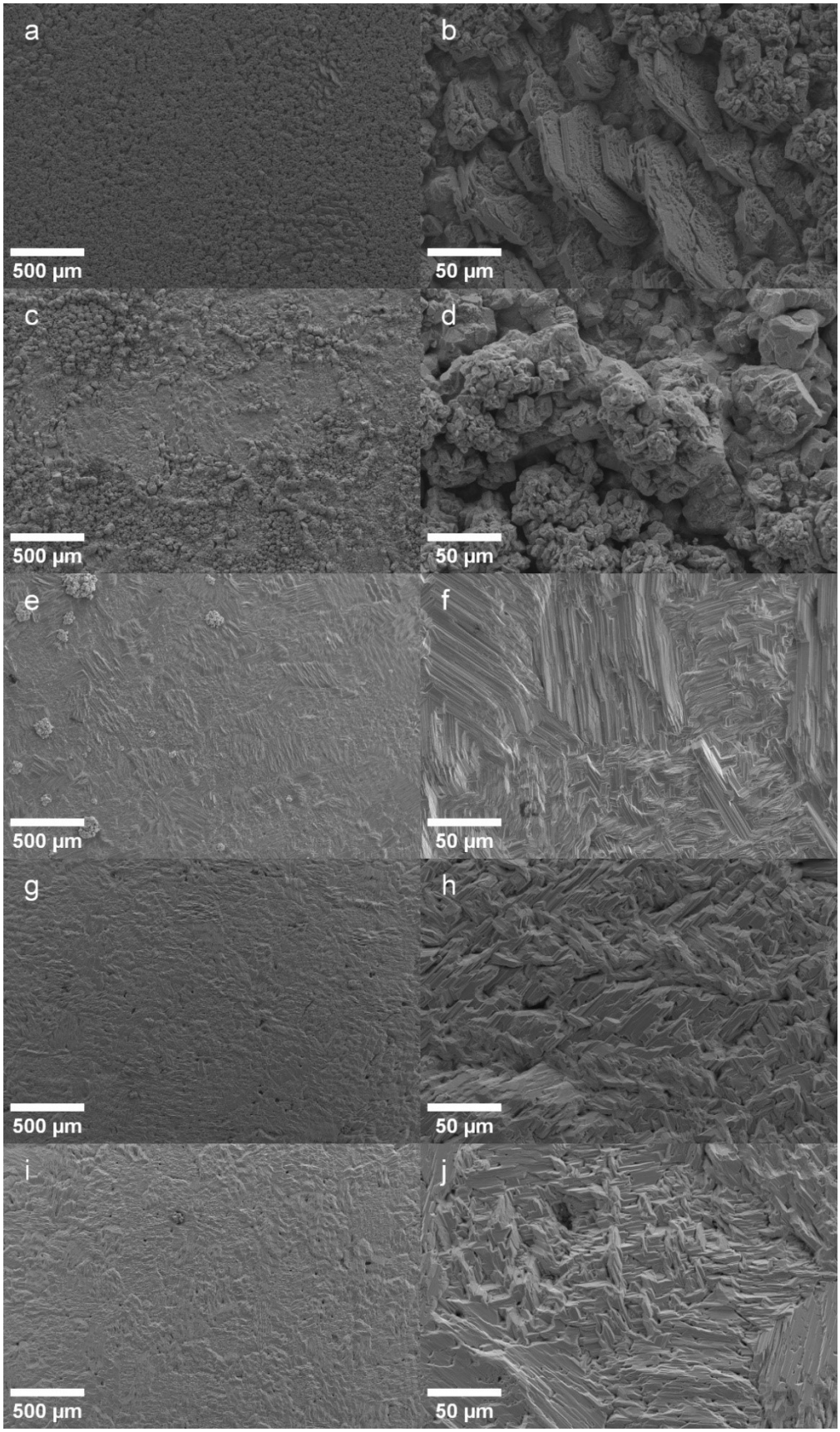

Supplementary Figure 13. SEM micrographs of Zn deposited over Sn current collector at a current density of **10 mA cm^{-2}** for 1h, taken at X100 and X1000 magnifications, respectively: from (a)+(b) Ref+1mM UPS solution; (c)+(d) Ref+5mM UPS solution; (e)+(f) Ref+10mM UPS solution; (g)+(h) Ref+15mM UPS solution; (i)+(j) Ref+20mM UPS solution.

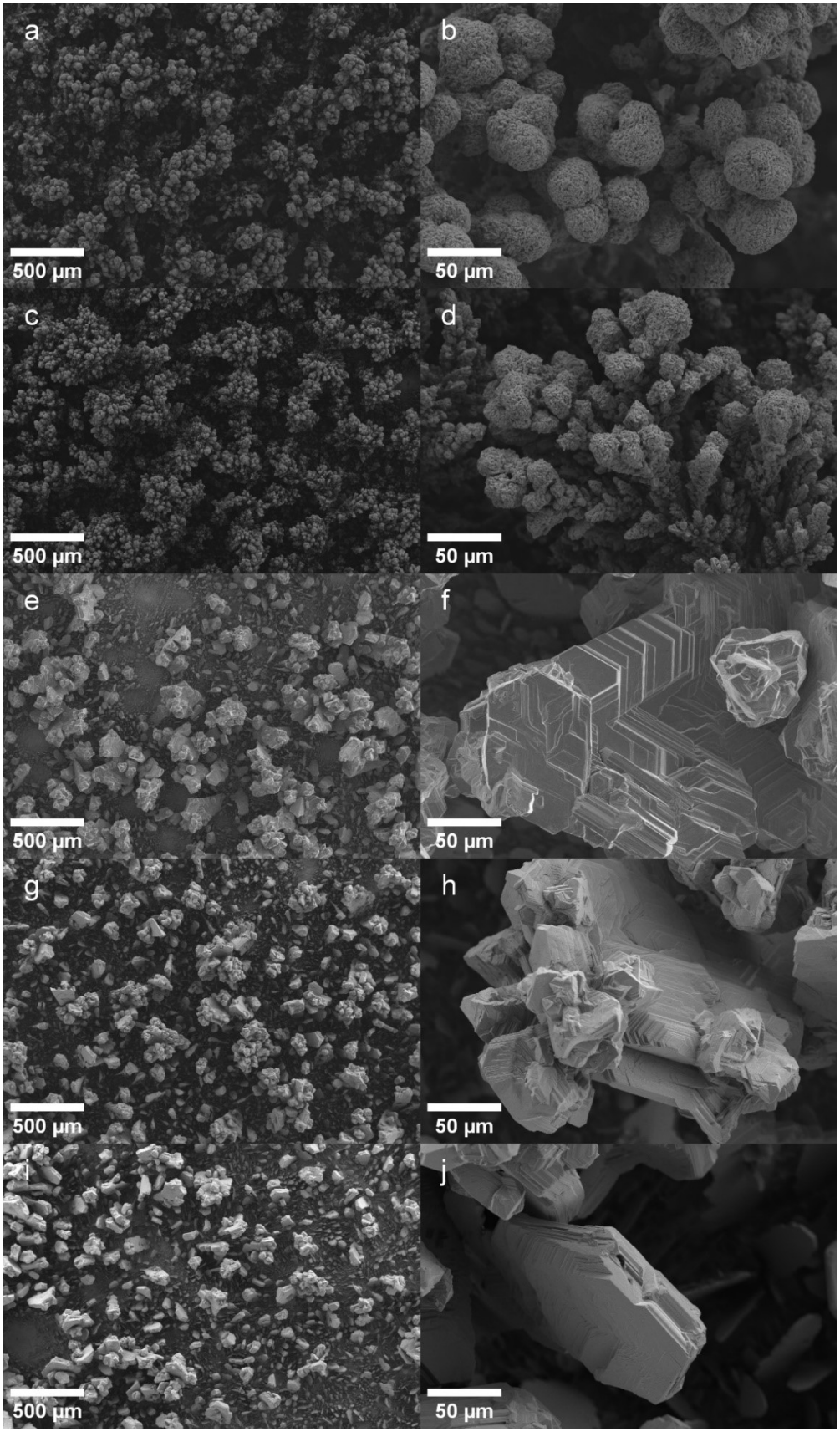

Supplementary Figure 14. SEM micrographs of Zn deposited over Sn current collector at a current density of **15 mA cm^{-2}** for 1h taken at X100 and X1000 magnifications, respectively: (a)+(b) from Ref+1mM UPS solution; (c)+(d) Ref+5mM UPS solution; (e)+(f) Ref+10mM UPS solution; (g)+(h) Ref+15mM UPS solution; (i)+(j) Ref+20mM UPS solution.

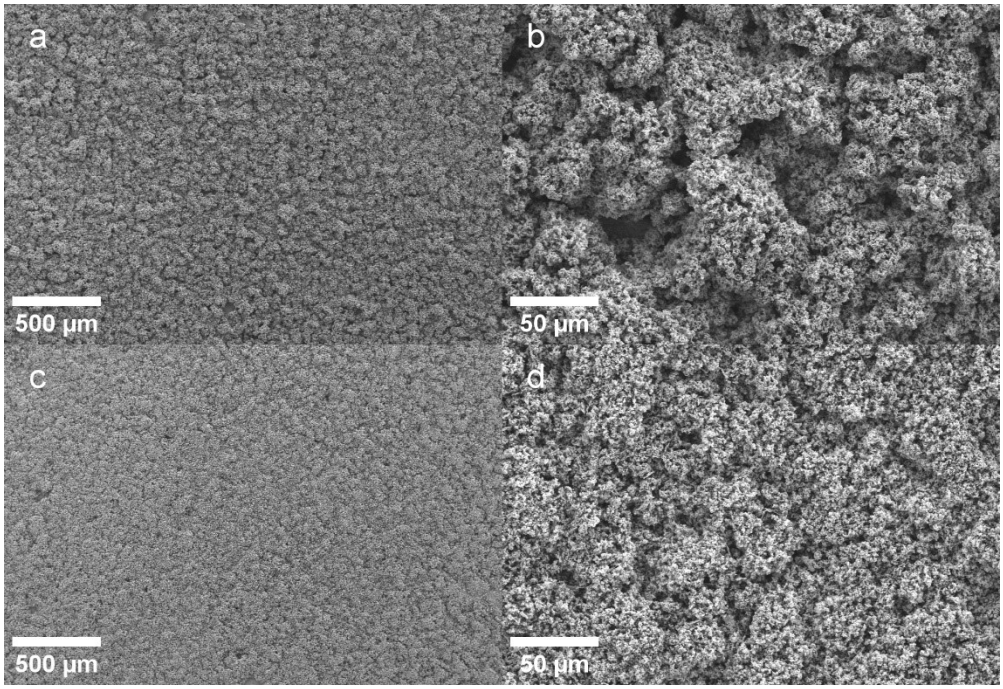

Supplementary Figure 15. SEM micrographs of Zn deposited over Sn current collector at a current density of **5 mA cm^{-2}** for 1h taken at X100 and X1000 magnifications, respectively: (a)+(b) from Ref+1mM DPS solution; (c)+(d) from Ref+5mM DPS solution.

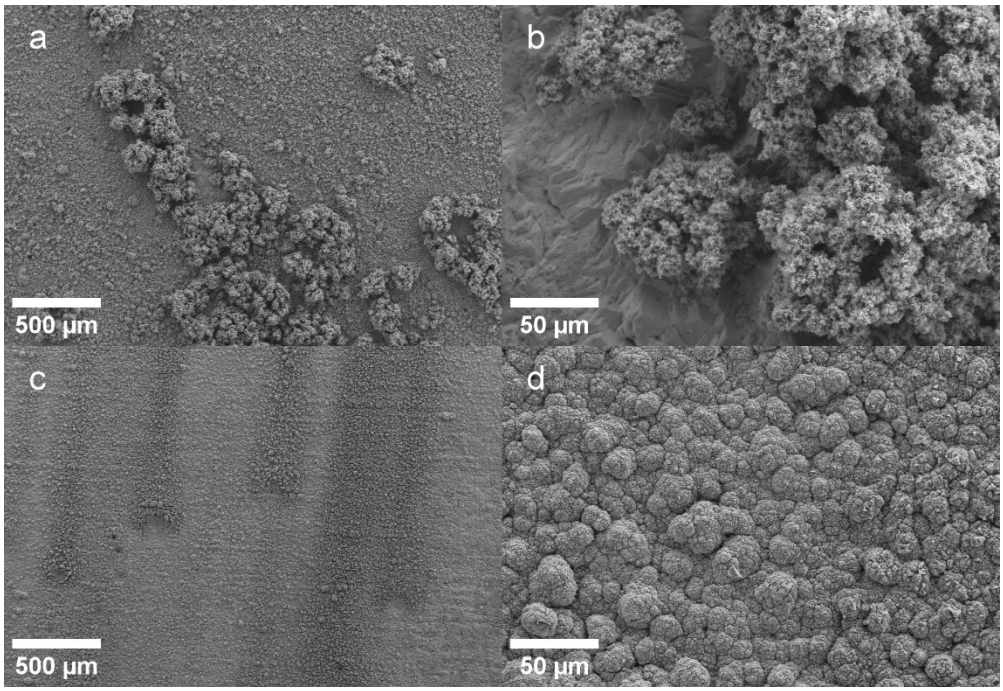

Supplementary Figure 16. SEM micrographs of Zn deposited over Sn current collector at a current density of **10 mA cm^{-2}** for 1h taken at X100 and X1000 magnifications, respectively: (a)+(b) from Ref+1mM DPS solution; (c)+(d) from Ref+5mM DPS solution.

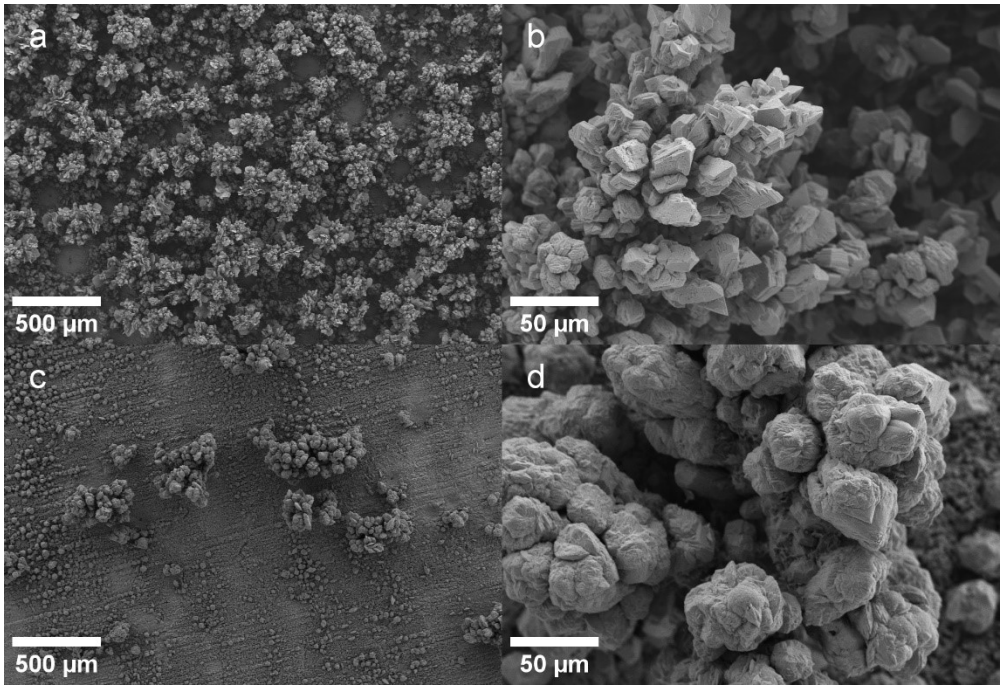

Supplementary Figure 17. SEM micrographs of Zn deposited over Sn current collector at a current density of 1**5 mA cm^{-2}** for 1h taken at X100 and X1000 magnifications, respectively: (a)+(b) from Ref+1mM DPS solution; (c)+(d) from Ref+5mM DPS solution.

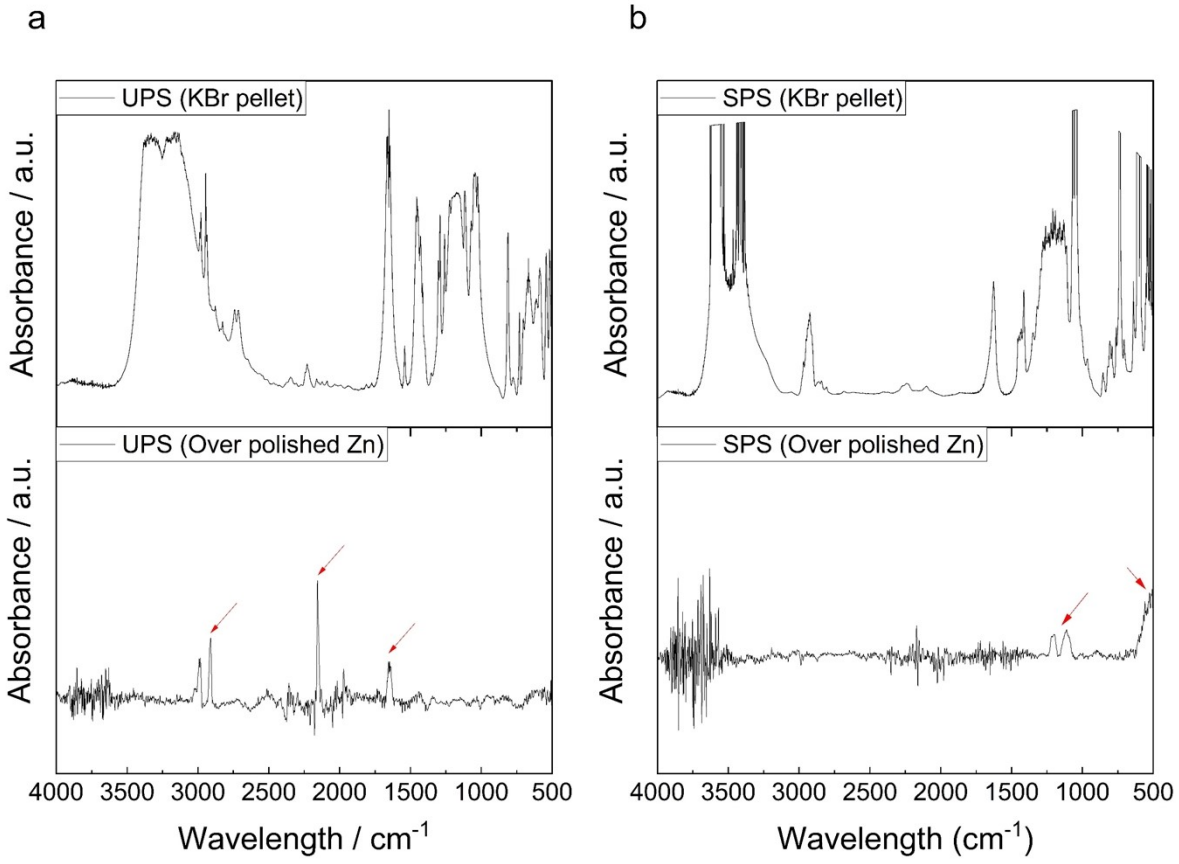

Supplementary Figure 18 FTIR absorbance spectra for dry additive pellet and adsorbed additive on top of Zn foils after 2h immersion in concentrated alkaline additive solution: (a) UPS and (b) SPS

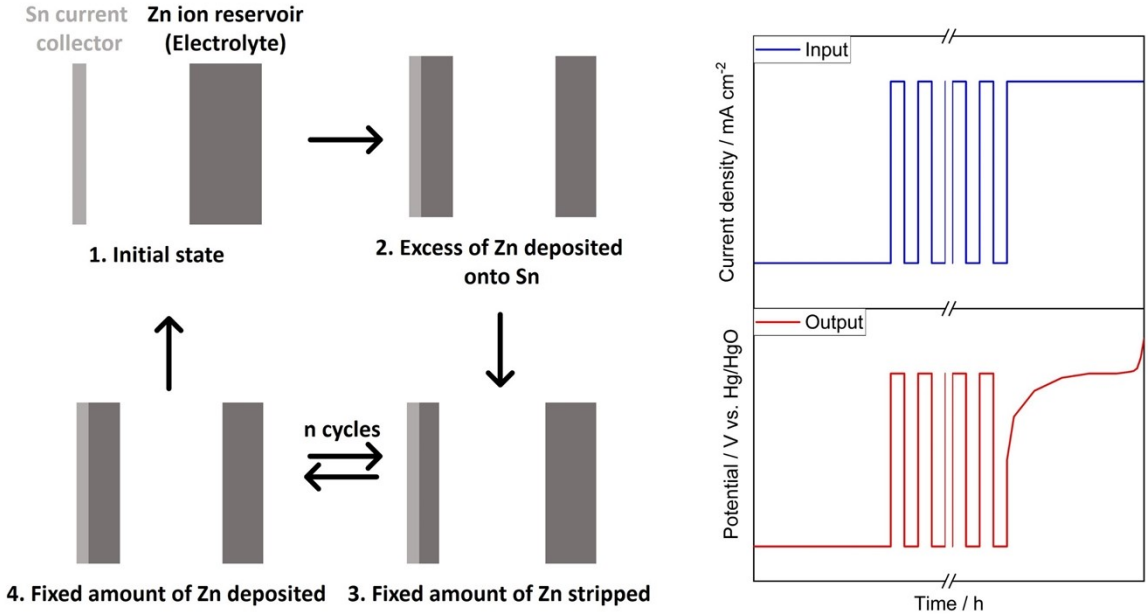

Supplementary Figure 19. Schematic diagram of cycling Zn anode half cells (i.e. Zn‖Pt) with constant current to determine the CE with illustration of the input signal and output measured data.

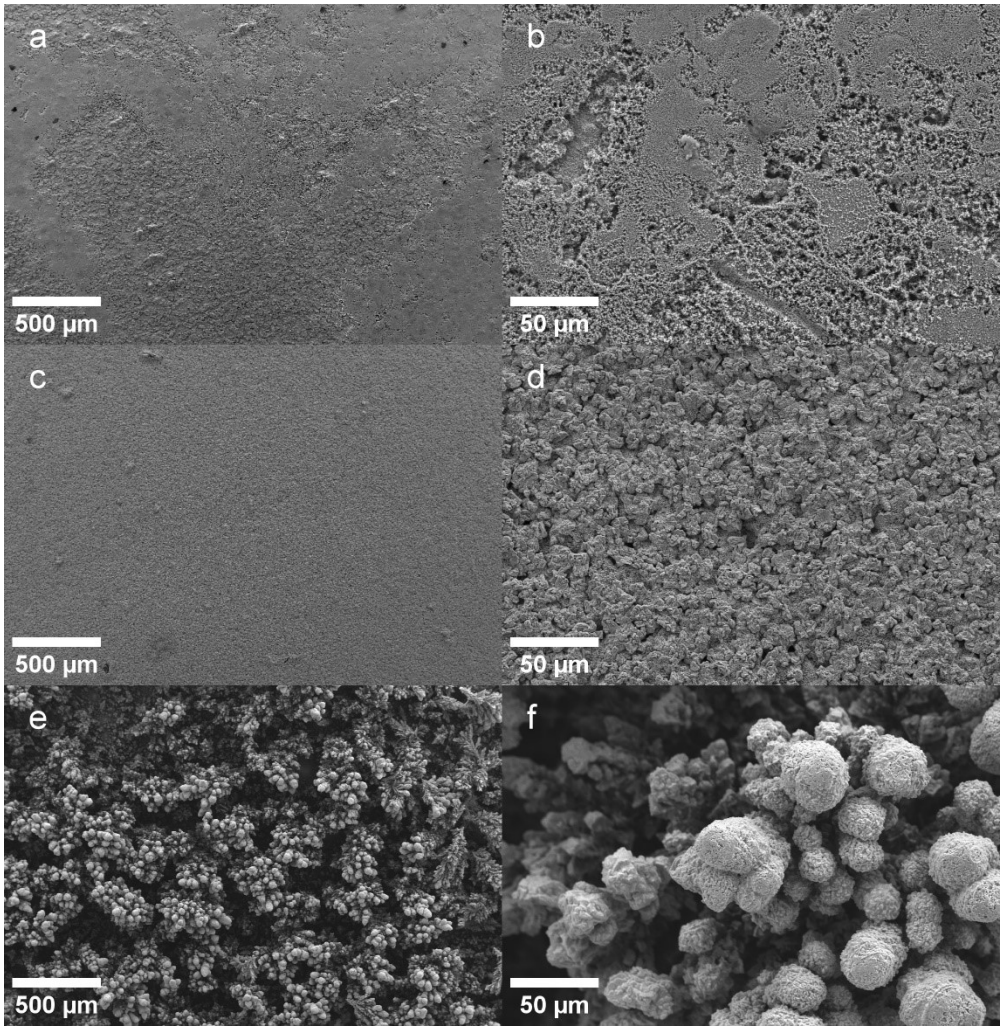

Supplementary Figure 20. SEM micrographs of Zn deposit over Sn current collector; Zn was deposited for 1 h from 15mM UPS+5mM SPS -modified electrolyte at current density of (a)+(b) 5 mA cm^{-2}; (c)+(d) 10 mA cm^{-2}; (e)+(f) 15 mA cm^{-2}. Images are taken at X100 and X1000 magnifications, respectively.

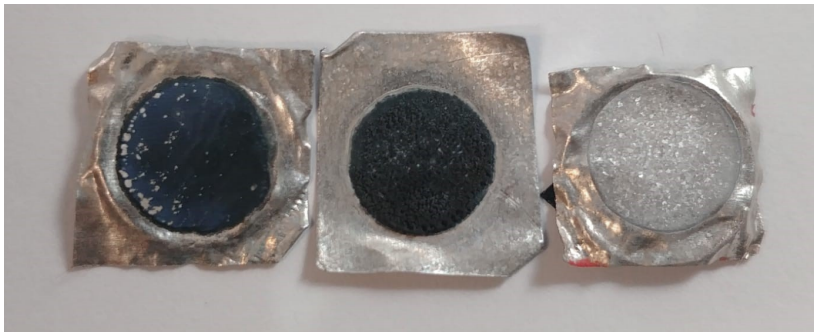

Supplementary Figure 21. On the left - visually obtained deposit from 20mM UPS+800ppm PEGdA600 modified electrolyte, in the middle – visual representation of surface covered by voluminous moss and on the right illustration of surface covered by compact layer-like deposit.

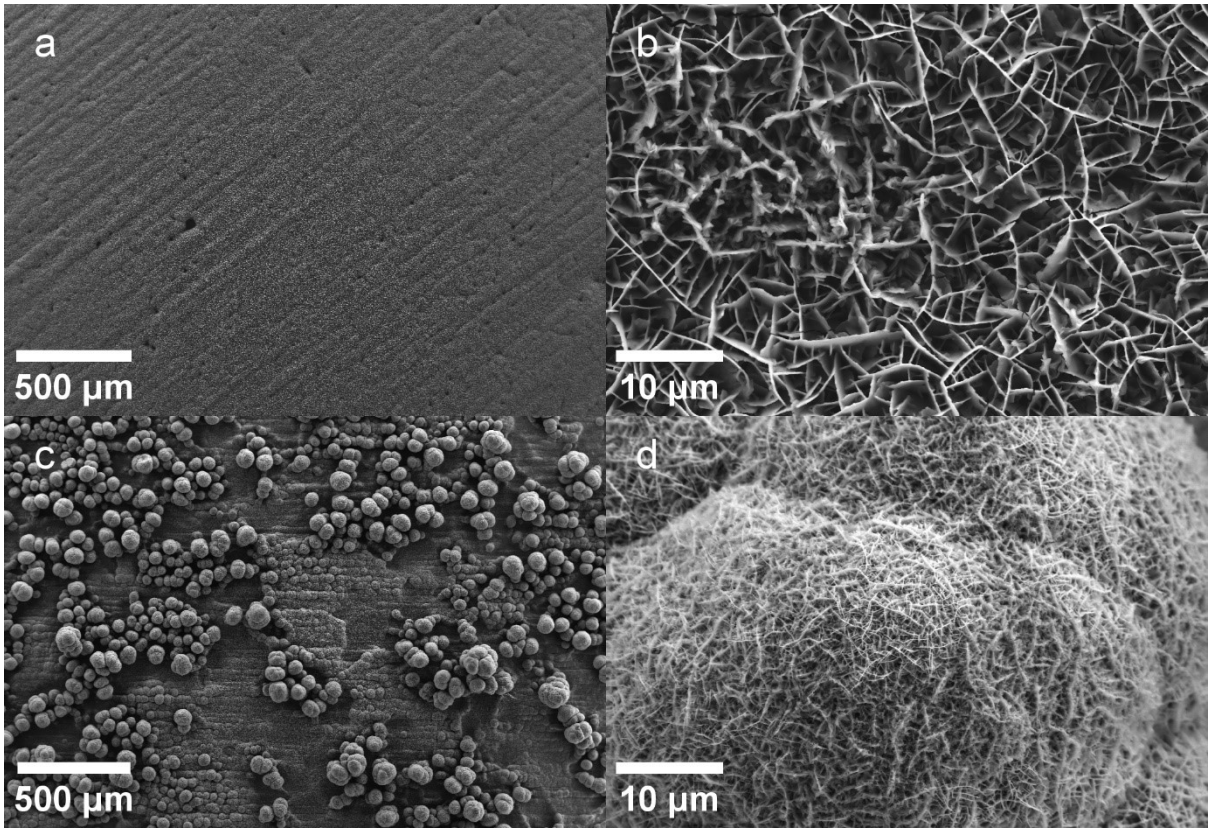

Supplementary Figure 22. SEM micrographs of Zn deposit over Sn current collector. Zn was deposited at a current density of 10 mA cm^{-2} for 1h, taken at X100 and X5000 magnifications, respectively. Deposition was made from: (a)+(b) Ref+20mM UPS+50ppm PEGdA600 solution; (c)+(d) Ref+20mM UPS+10ppm PEGdA600 solution.

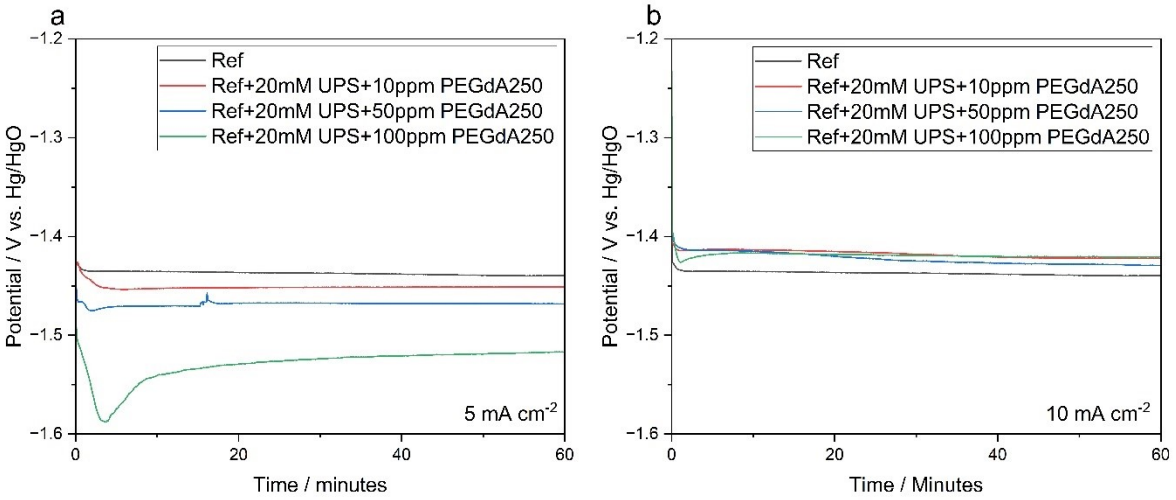

Supplementary Figure 23. Chronopotentiometry profiles in additive-free electrolyte and 20mM UPS+different concentrations of PEGdA250 -modified electrolytes at current densities of: (a) 5 mA cm^{-2} and (b) 10 mA cm^{-2}.

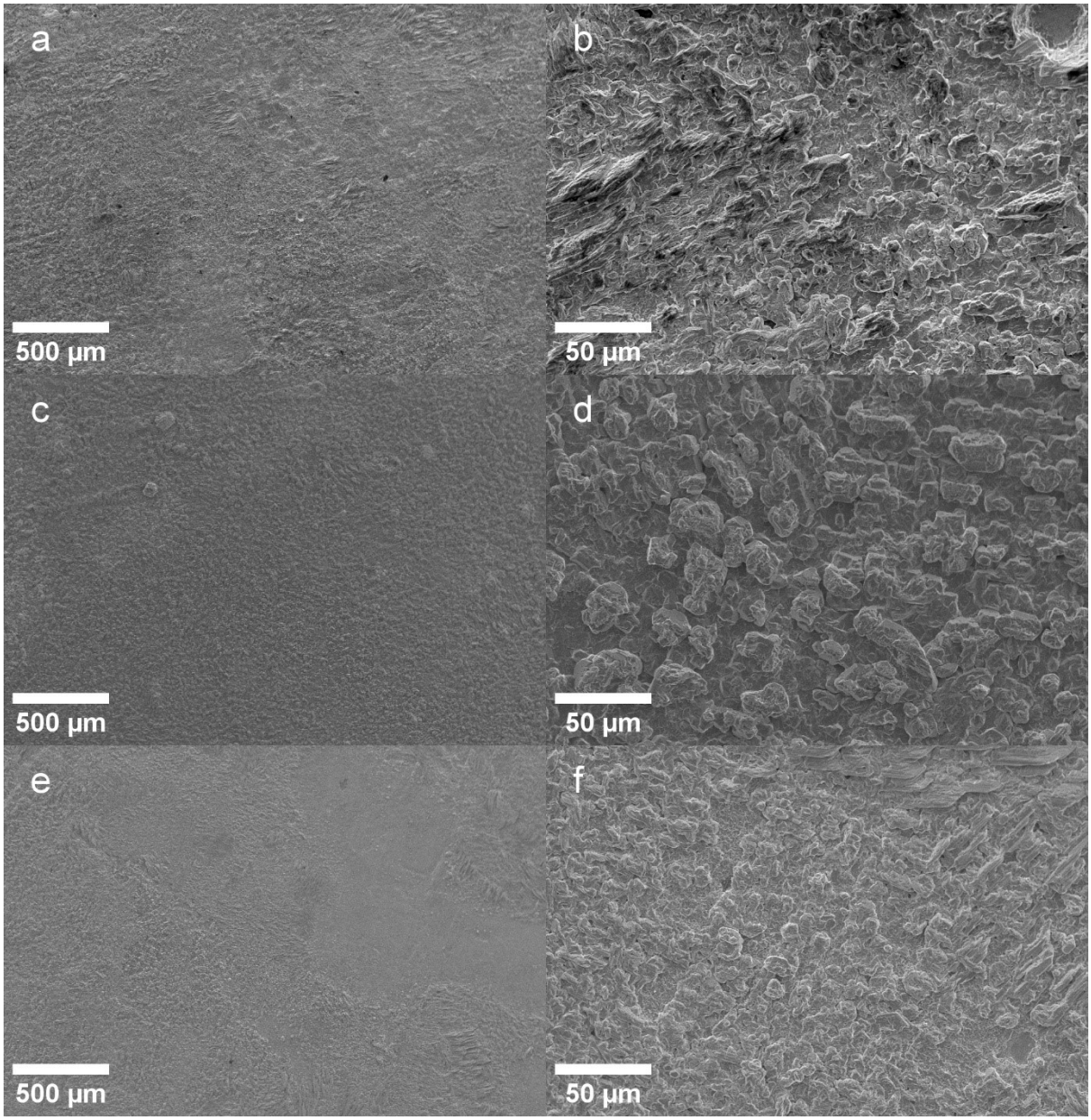

Supplementary Figure 24. SEM micrographs of Zn deposit over Sn current collector; Zn was deposited at a current density of 5 mA cm^{-2} for 1h from: (a)+(b) Ref+20mM UPS+10ppm PEGdA250 solution; (c)+(d) Ref+20mM UPS+50ppm PEGdA250 solution, and (e)+(f) Ref+20mM UPS+100ppm PEGdA250 solution. Images were taken at X100 and X1000 magnifications, respectively.

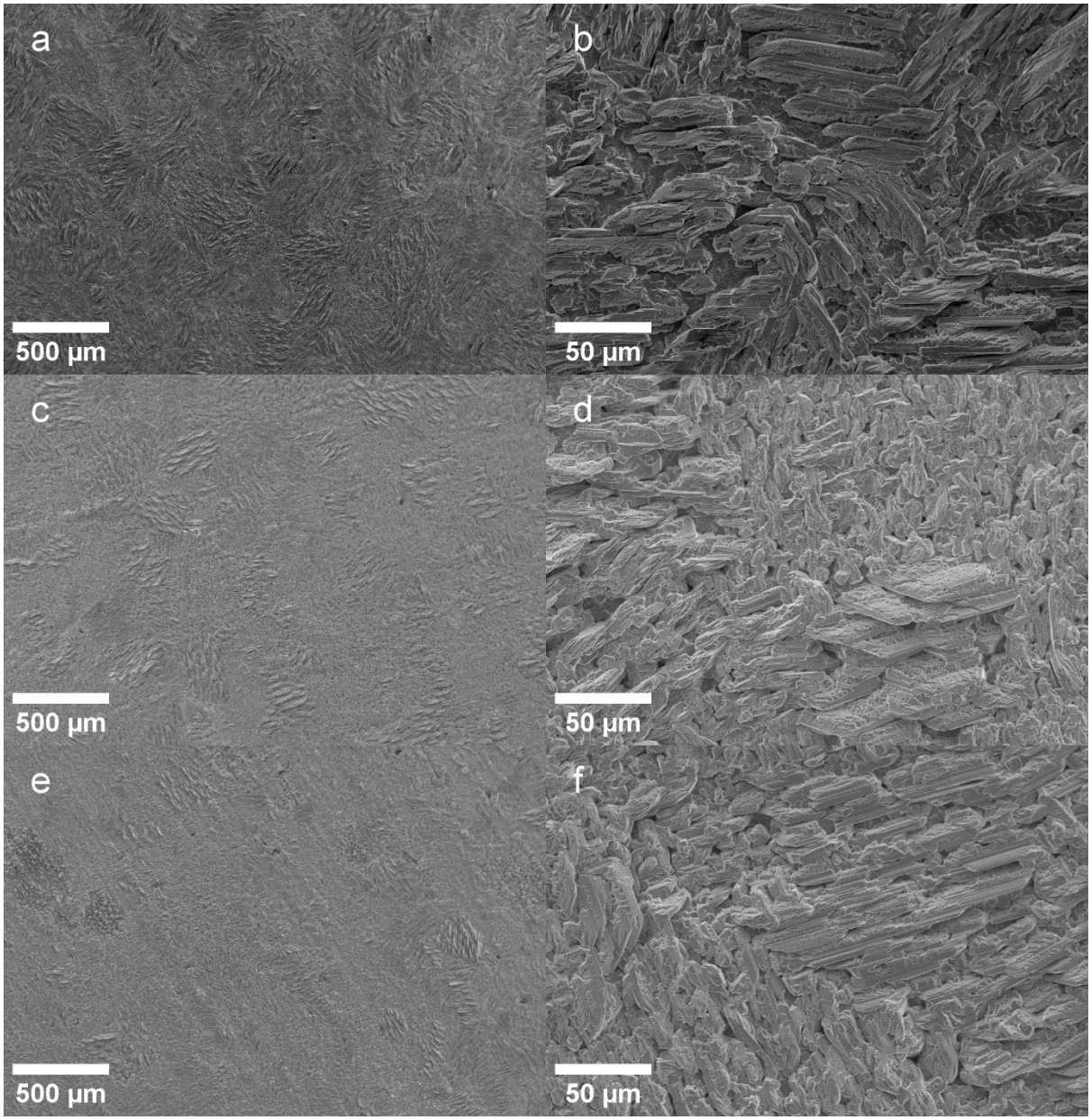

Supplementary Figure 25. SEM micrographs of Zn deposit over Sn current collector. Zn was deposited at current density of 10 mA cm^{-2} for 1h from: (a)+(b) Ref+20mM UPS+10ppm PEGdA250 solution; (c)+(d) Ref+20mM UPS+50ppm PEGdA250 solution, and (e)+(f) Ref+20mM UPS+100ppm PEGdA250 solution. Images were taken at X100 and X1000 magnifications, respectively.

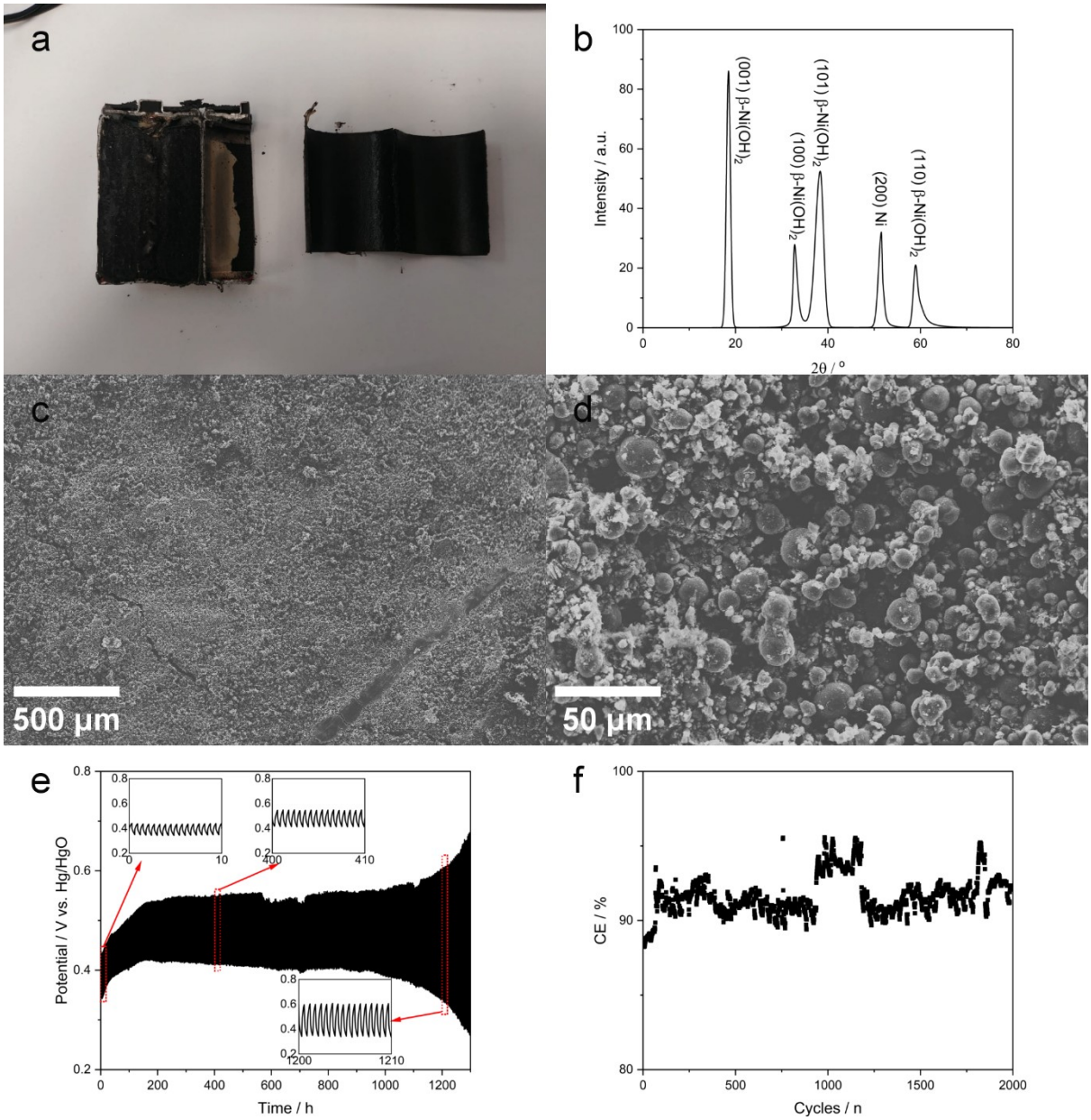

Supplementary Figure 26. (a) Ansmann d-cell battery cross-section and extracted cathode; (b) XRD difractogram of the extracted, washed and dried $Ni(OH)_2$ cathode, and SEM micrographs of the $Ni(OH)_2$ cathode in top-view at: (c) X100 magnification and (d) X1000 magnification; (e) GCDC of $Ni(OH)_2$‖Pt half-cell in a pristine additives-free electrolyte; (f) CE (%) of the cycled cathode.

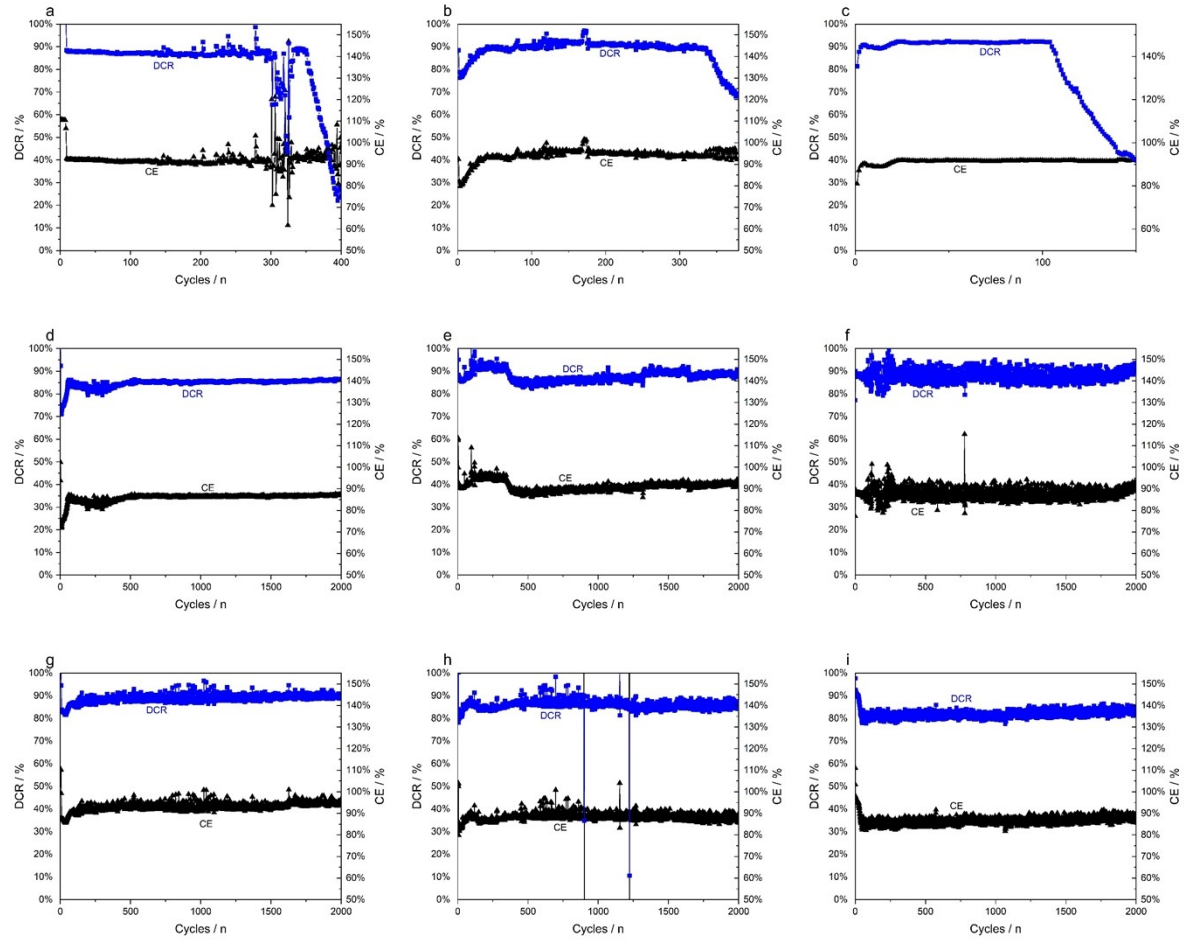

Supplementary Figure 27. Discharge capacity retention % and coulombic efficiency % determined according to the data obtained via GCDC. **(a-c) an additive-free electrolyte:** (a) 50%DoD, (b) 80%DoD and (c) 100% DoD; **(d-f) 20mM UPS-modified electrolyte:** (d) 50%DoD, (e) 80%DoD and (f) 100% DoD; **(g-i) 20mM UPS+50ppm PEGdA250 modified electrolyte**: (g) 50%DoD, (h) 80%DoD and (i) 100% DoD.

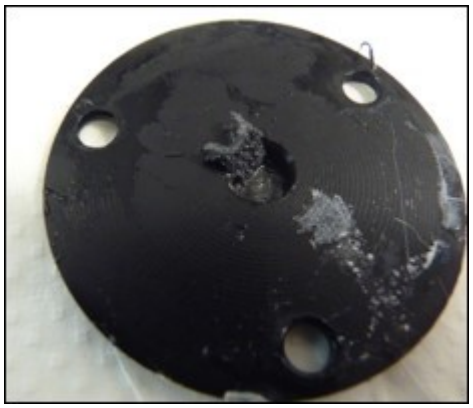

Supplementary Figure 28. Sludge formed on the anode while performing GCDC from a pristine additives-free electrolytes.

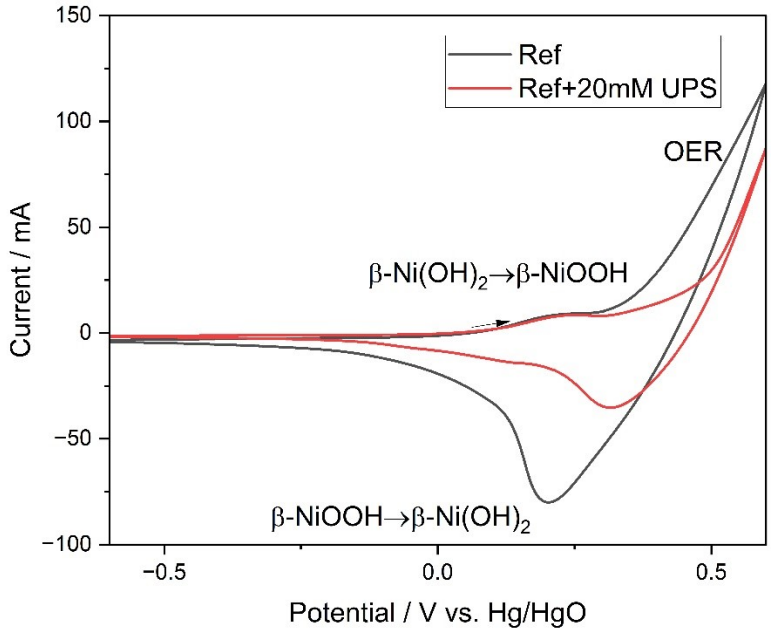

Supplementary Figure 29. CV of $Ni(OH)_2$‖Pt Half-cell in pristine and UPS- modified electrolytes – swept at 1mV s^{-1} rate, starting from OCP, scanned anodically to 0.5V $_{vs.\ Hg/HgO}$, then scanned back cathodically up to -0.7V $_{vs.\ Hg/HgO}$ and back to OCP.

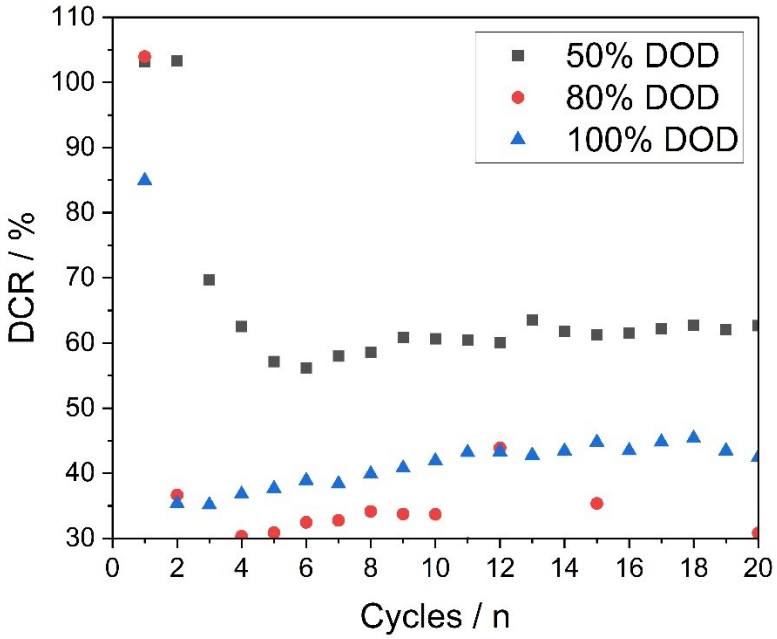

Supplementary Figure 30. GCDC for electrolytes modified solely by PEGdA250; same conditions as previously.

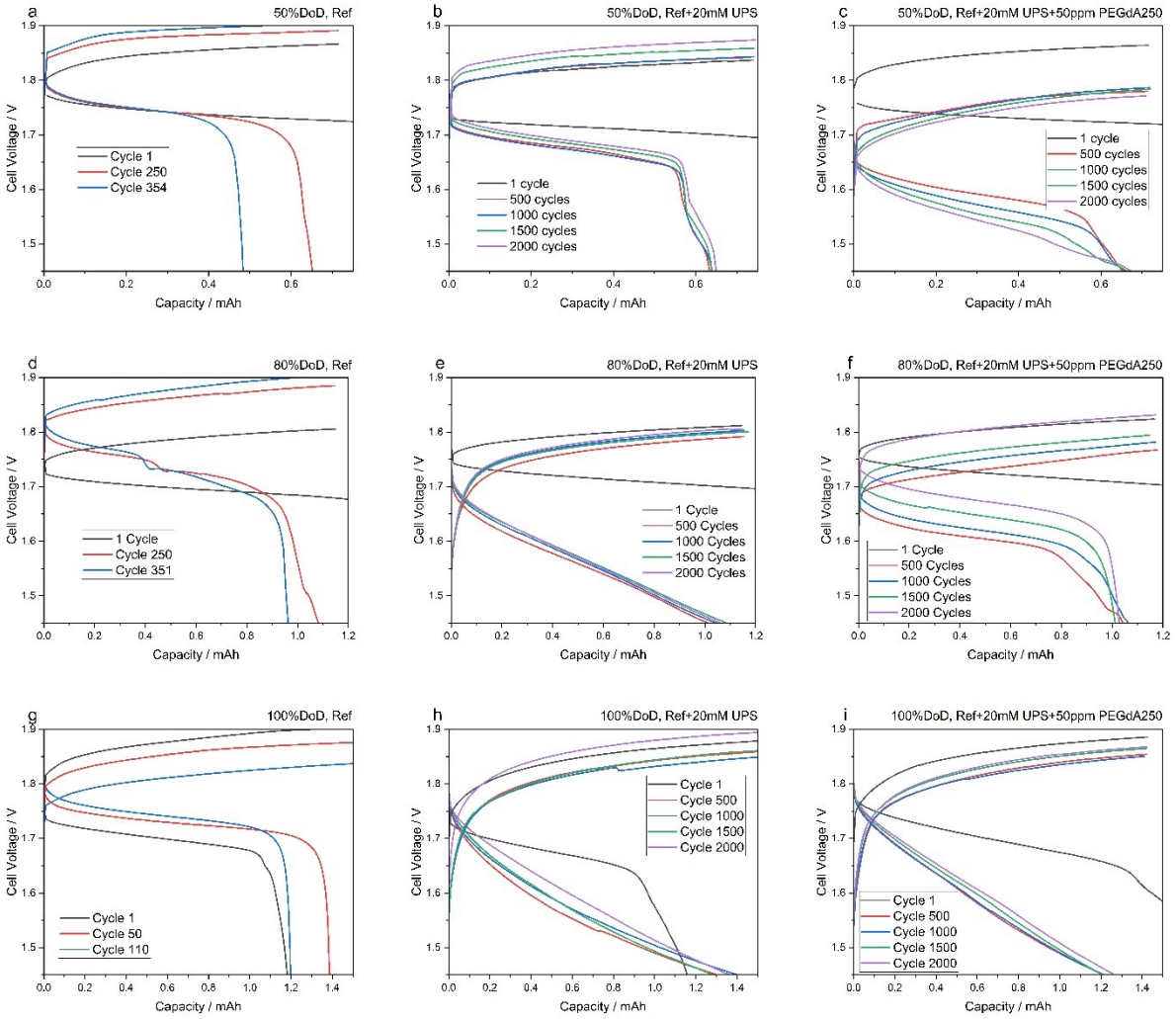

Supplementary Figure 31. Cell voltage versus charging and discharging capacity during GCDC – DoD of; (a)-(c) 50%, (d)-(f) 80% and (g)-(i) 100%. Profiles were recorded from cells cycled in an additives-free pristine electrolyte, 20mM UPS-modified electrolyte and 20mM UPS+50ppm PEGdA250- modified electrolyte, respectively.

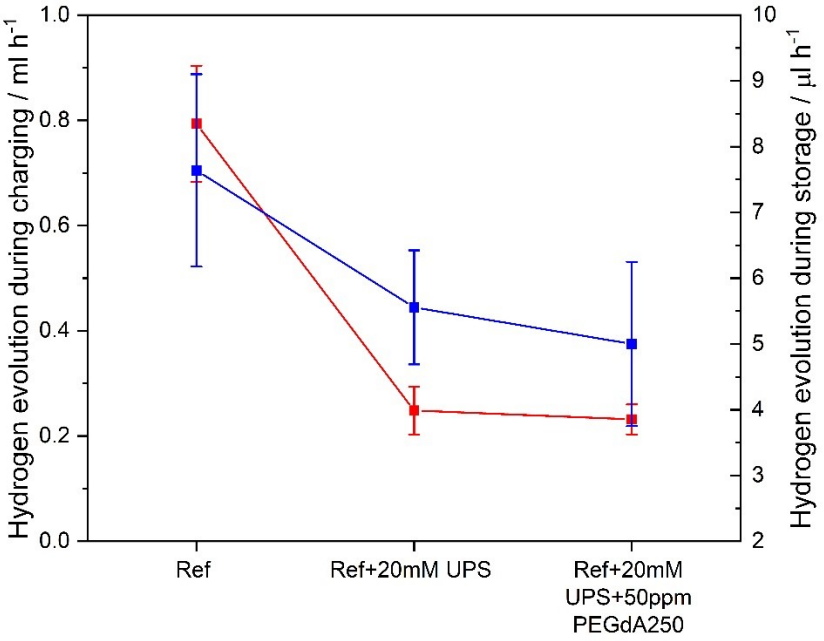

Supplementary Figure 32. Hydrogen evolution rate during charging (red curve) and during storage (blue curve)

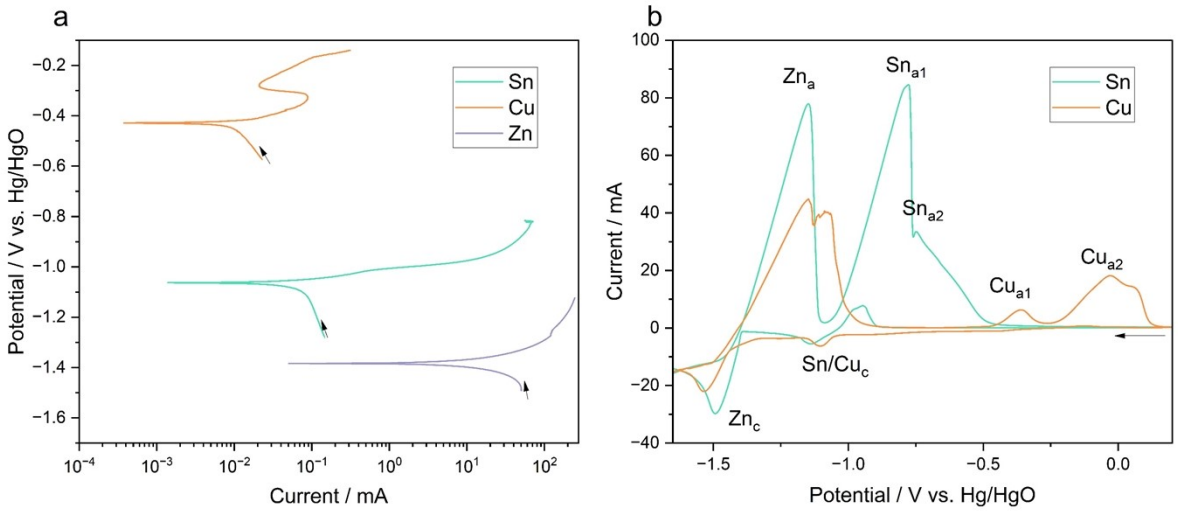

Supplementary Figure 33. (a) Linear scanning voltammetry of different current collectors in pristine solution (sweep rate of 0.125mV s^{-1}), (b) Cyclic voltammetry of Sn and Cu current collectors in pristine solution (sweep rate of 10mV s^{-1}).

According to prior studies dealing with Zn deposition from alkaline media on top of different substrates [1–3], Cu or Sn were appropriate choices for the current collector. Due to a minor crystallographic mismatch between the Zn basal plane and the close-packed plane of Cu, Zn deposition over Cu generates minimal nucleation overpotential, and the produced deposit is parallel to basal planes, resulting in very small grains. However, underpotential deposition, formation of brass alloys, and a sufficiently higher exchange current for hydrogen reduction are also feasible. Unlike Cu, there is no indication of underpotential deposition or alloy formation on Sn. It also has a comparable exchange current for hydrogen evolution to that of Zn and a low charge transfer resistance.

Preliminary tests showed that the corrosion rate in the pristine electrolyte reduced in the following order: Zn>Sn>Cu, as shown in Fig. S33 (a). As seen in Fig. S33 (b), the cathodic shift for Zn deposition on Cu was greater than that for Sn, suggesting that Sn is a more facile substrate in terms of overpotential for Zn deposition in this specific electrolyte. Furthermore, the obtained CV suggests that some underpotential deposition occurs on top of Cu, as seen from the shoulder before to the cathodic Zn deposition peak and supports the results of previously mentioned studies. Overall, the reversibility of Zn deposition over the Sn substrate is more prominent and the overall kinetics are faster as demonstrated by currents.

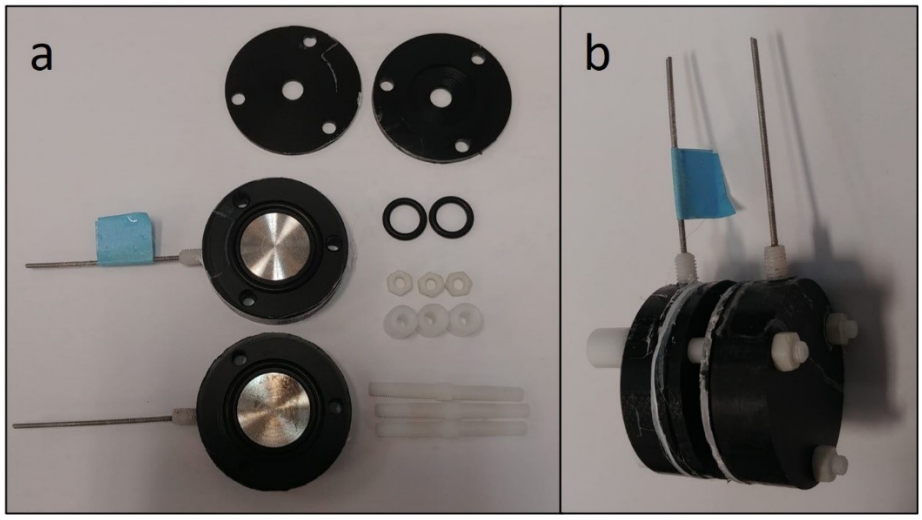

Supplementary Figure 34. Illustration of the cell configuration, used as half cell with Pt CE and Hg/HgO RE or as full cell with the $Ni(OH)_2$ Cathode.

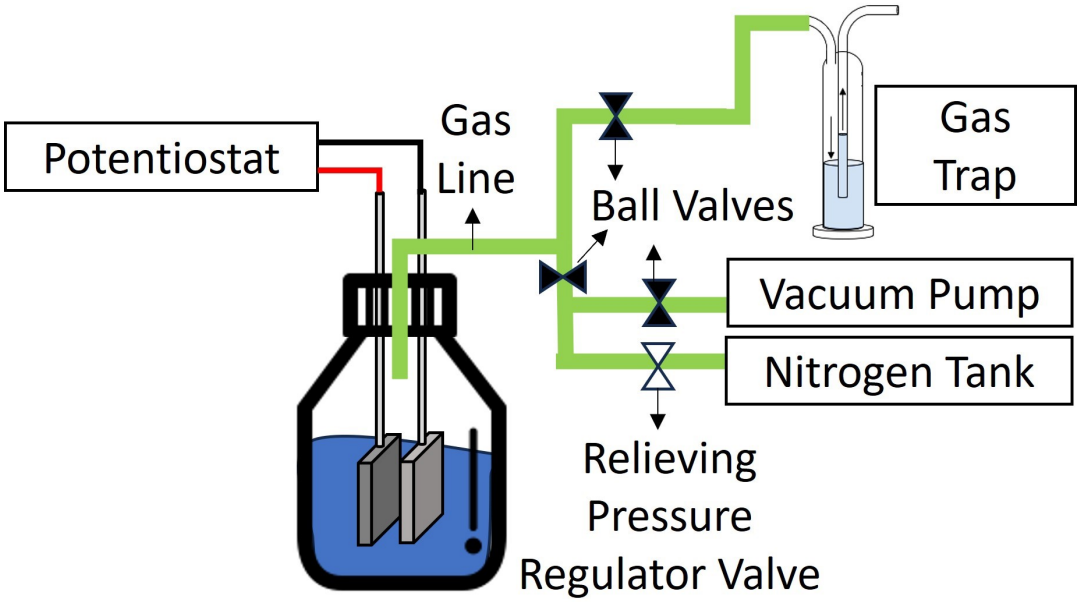

Supplementary Figure 35. Scheme of gas collection cell and system.

References to the supplementary material

1 M. G. Chu, J. McBreen and G. Adzic, *J. Electrochem. Soc.*, 1981, **128**, 2281.

2 J. McBreen, M. G. Chu and G. Adzic, *J. Electrochem. Soc.*, 1981, **128**, 2287.

3 X. Wei, D. Desai, G. G. Yadav, D. E. Turney, A. Couzis and S. Banerjee, *Electrochim. Acta*, 2016, **212**, 603.